Supporting Information for

A potential shift from a carbon sink to a source in Amazonian peatlands under a changing climate

[1]Sirui Wang, [1]Qianlai Zhuang, [2]Outi Lähteenoja, [3,4]Frederick C Draper, and [2]Hinsby Cadillo-Quiroz

[1]Department of Earth, Atmospheric & Planetary Sciences and Department of Agronomy, Purdue University, West Lafayette, IN, USA

[2]School of Life Sciences, Arizona State University, Tempe, AZ, USA

[3]Department of Global Ecology, Carnegie Institution of Science, Stanford, CA, USA

[4]International Center for Tropical Botany, Florida International University, Miami, FL, USA

*Correspondence to: qzhuang@purdue.edu

Contents of this file

www.pnas.org/cgi/doi/10.1073/pnas.1801317115

Model Description and Parameterization

1. Peat Soil Organic Carbon Accumulation

Peat soil organic carbon (SOC) accumulation is determined by the net primary production (NPP) and aerobic and anaerobic respiration[1] based on the core C and nitrogen dynamic module for upland ecosystems[2]. The net ecosystem production (NEP) for the peatland ecosystem is calculated at a monthly step:

$$\mathrm{NEP} = \mathrm{NPP} - R_H - R_{CH_4} - R_{CWM} - R_{CM} - R_{COM}$$

where NPP represents the monthly net primary production. R_H represents the monthly aerobic respiration related to the variability of water table depth, soil moisture, soil temperature, and soil organic C. R_{CH_4} represents the monthly methane emission after methane oxidation. R_{CWM} represents the CO_2 emission due to methane oxidation[3]. R_{CM} represents the CO_2 release accompanied with the methanogenesis[4]. R_{COM} represents the CO_2 release from other anaerobic processes (e.g., fermentation and terminal electron acceptor reduction)[5].

1.1 Net Primary Production (NPP)

Gross primary production (GPP) is defined as the total assimilation of CO_2-C by plants, excluding photorespiration. GPP is modeled as a function of the irradiance of photosynthetically active radiation (PAR), atmospheric CO_2 concentrations, moisture availability, mean air temperature, the relative photosynthetic capacity of the vegetation, and nitrogen availability (see[6] for details):

$$\text{GPP} = (C_{max})\frac{PAR}{k_i + PAR}\frac{C_i}{k_c + C_i}f(PHENOLOGY)f(FOLIAGE)f(T)f(NA)$$

where C_{max} is the monthly maximum rate of C assimilation by the entire plant canopy under optimal environmental conditions (g m^{-2} $month^{-1}$); PAR is the irradiance of photosynthetically active radiation at canopy level (J cm^{-2} day^{-1}); k_i is the irradiance at which C assimilation proceeds at one-half its maximum rate; C_i is the concentration of CO_2 inside leaves (mL L^{-1}); k_c is the internal CO_2 concentration at which C assimilation proceeds at one-half its maximum rate. $f(PHENOLOGY)$ is monthly leaf area relative to leaf area during the month of maximum leaf area and depends on monthly estimated evapotranspiration[6]. $f(FOLIAGE)$ is a scaler function that ranges from 0.0 to 1.0 and represents the ratio of canopy leaf biomass relative to maximum leaf biomass. T is monthly air temperature and NA is nitrogen availability. The function $f(NA)$ models the limiting effects of plant nitrogen status on GPP.

Moisture limitations on CO_2 assimilation is modeled by the modifying the conductance of leaves to CO_2 diffusion. The mean monthly moisture availability is the degree to which environmental demands for water are met by rainfall and available soil moisture. This is expressed as the ratio of actual evapotranspiration (*EET*) to potential evapotranspiration (*PET*). We assume that the relationship between CO_2 concentration inside stomatal cavities (C_i) and in the atmosphere (C_a) is proportional to relative moisture availability:

$$G_V = 0.1 + (\frac{0.9EET}{PET})$$

and

$$C_i = G_V C_a$$

where G_V is relative canopy conductance, a unitless multiplier that accounts for changes in leaf conductivity to CO_2 resulting from changes in moisture availability. When moisture is not limiting, G_V is close to 1.0 and CO_2 inside leaves will be close to ambient CO_2.

Temperature effect on GPP is modeled as a multiplier on potential GPP, with a maximum value of 1 at the optimum temperature and lower values at suboptimal temperatures:

$$f(T) = \frac{(T - T_{min})(T - T_{\mathrm{max}})}{(T - T_{min})(T - T_{max}) - \left(T - T_{opt}\right)^2}$$

where $f(T)$ is the unitless multiplier on GPP and T is the mean monthly air temperature (°C).

The phenological model was developed for simulating the changes seasonal changes in the vegetation's capacity to assimilate C. It models relative changes in the photosynthetic capacity of mature vegetation (*KLEAF*) from estimated actual evapotranspiration (*EET*) and the previous month's photosynthetic capacity:

$$f(PHENOLOGY)_j = a\left(\frac{EET_j}{EET_{max}}\right) + b\left(f(PHENOLOGY)_{j-1}\right) + c$$

$$f(PHENOLOGY)_j = 1$$

$$(\text{if } f(PHENOLOGY)_j > 1)$$

$$f(PHENOLOGY)_j = \frac{f(PHENOLOGY)_t}{f(PHENOLOGY)_{max}}$$

$$(\text{if } f(PHENOLOGY)_j < 1)$$

The time step j is one month; EET_{max} is the maximum *EET* occurring during any month; a, b, and c are regression-derived parameters.

Plant (autotrophic) respiration (R_A) is the total respiration (excluding photorespiration), including all CO_2 production from the various processes of plant maintenance, nutrient uptake, and biomass construction. R_A is the sum of maintenance respiration (R_m), and growth respiration (R_g):

$$R_A = R_m + R_g$$

The maintenance respiration is modeled as a direct function of plant biomass (C_V).We assume that increasing temperatures increase maintenance respiration logarithmically with a Q_{10} of 2 over all temperatures:

$$R_m = K_r(C_V)e^{0.0693T}$$

where K_r is the respiration rate of the vegetation per unit of biomass carbon at 0°C ($\mathrm{g\,g^{-1}\,month^{-1}}$), and T is the mean monthly air temperature (°C). Growth or construction respiration R_g is estimated to be 20% of the difference between GPP and R_m:

$$\mathrm{NPP'_t} = \mathrm{GPP_t} - R_{mt}$$

$$R_{gt} = 0.2\mathrm{NPP'_t}$$

where $\mathrm{NPP'}$ is the potential net primary production assuming that the conversion efficiency of photosynthate to biomass is 100% and *t* refers to the monthly time step.

Net primary production (NPP) is the difference between GPP and autotrophic respiration (R_{At}):

$$\mathrm{NPP_t} = \mathrm{GPP_t} - R_{At}$$

NPP is calibrated to correctly estimate annual NPP since monthly observed NPP do not exit for most vegetation types from the field measurements.

Nitrogen availability influences GPP individually by influencing the relative allocation of effort toward C vs. nitrogen uptake (Ac). See[6] for details in Carbon-Nitrogen interaction model.

1.2 Aerobic Respiration Related to Water Table Depth (R_H)

SOC aerobic respiration related to the variability of water table depth (R_H) is calculated as:

$$R_H = K_d C_{s1} f(M_V) e^{0.069 H_T} \frac{WTD}{LWB}$$

where M_V represents the mean monthly soil water content (percentage of saturation) in the peat unsaturated zone above the water table depth (WTD). K_d is a logarithm of heterotrophic rate at 0°C. H_T is the mean monthly temperature of the soil above the lowest water table boundary[7] (LWB, a fixed parameter, the soil below which is set saturated). The SOC between LWB and soil surface (C_{s1}) in the transient simulation is obtained after a 2000-year equilibrium run.

$f(M_V)$ is a non-linear function defining the influence of soil moisture on decomposition:

$$B = \left(\frac{M^{m1} - M_{opt}^{m1}}{M_{opt}^{m1} - 100^{m1}} \right)^2$$

$$f(M_V) = (0.8 M_{sat}^{B}) + 0.2$$

where $m1$ is a parameter defining the skewness of the curve. M_{opt} is the soil moisture content at which $f(M_V)$ is maximum (1.0). M_{sat} is a parameter that determines the value of $f(M_V)$ when the soil pore space is saturated with water.

The peatland soil is modeled as a two-layer system[6]. The soil layers above the LWB are divided into 1 cm sublayers, where peat soil characteristics in the upper peat are constant above 7 cm peat depth and change linearly in the section interval of 1 cm below the *WTD*. The *WTD* is estimated based on the total amount of water content above the LWB within the upper two soil layers. Using the calculated *WTD*, the water content at each 1 cm above the *WTD* can be determined after solving the water balance equations.

1.3 R_{CH_4}, R_{CWM}, R_{CM}, and R_{COM}

R_{CH_4} represents the monthly methane emission after methane oxidation (see[8] for details):

$$R_{CH_4} = M_P - M_O$$

where M_P is the monthly methane production /methanogenesis and M_O is the monthly methane oxidation.

M_P is modeled as an anaerobic process that occurs in the saturated zone of the soil profile. It is calculated as the integration of the hourly methanogenesis ($M_P(z,t)$) at each 1-cm layer:

$$M_P = \int_{t=1}^{24\times 30} \int_{z=1}^{100} M_P(z,t)\, dtdz$$

where

$$M_P(z,t) = M_{G0} f\big(S_{OM}(z,t)\big) f\big(M_{ST}(z,t)\big) f\big(pH(z,t)\big) f\big(R_X(z,t)\big)$$

M_{G0} is the ecosystem-specific maximum potential production rate; $f\big(S_{OM}(z,t)\big)$ is a multiplier that enhances methanogenesis with increasing methanogenic substrate availability, which is a function of net primary production of the overlying vegetation; $f\left(M_{ST}(z,t)\right)$ is a multiplier that enhances methanogenesis with increasing soil temperatures. $f\left(pH(z,t)\right)$ is a multiplier that diminishes methanogenesis if the soil-water pH is not optimal (i.e., pH=7.5). $f(R_X(z,t))$ is a multiplier that describes the effects of the availability of electron acceptors which is related to redox potential on methanogenesis.

M_O is modeled as the integration of hourly methane oxidation rate ($M_O(z,t)$) at each 1-cm layer:

$$M_O = \int_{t=1}^{24\times30} \int_{z=1}^{100} M_O(z,t)\, dtdz$$

where

$$M_O(z,t) = O_{MAX} f\left(C_M(z,t)\right) f\left(T_{SOIL}(z,t)\right) f\left(E_{SM}(z,t)\right) f(R_{OX}(z,t))$$

O_{MAX} is the ecosystem-specific maximum oxidation coefficient; $f\left(C_M(z,t)\right)$ is a multiplier that enhances methanotrophy with increasing soil methane concentrations; $f\left(T_{SOIL}(z,t)\right)$ is a multiplier that enhances methanotrophy with increasing soil temperatures; $f\left(E_{SM}(z,t)\right)$ is a multiplier that diminishes methanotrophy if the soil moisture is not at an optimum level; and $f(R_{OX}(z,t))$ is a multiplier that enhances methanotrophy as redox potentials increase.

R_{CWM} is the CO_2 emission due to methane oxidation; R_{CM} is the CO_2 release accompanied with methanogenesis. We assume the same amount of CO_2 is released along with the methane production (M_P). R_{COM} is the CO_2 release from other anaerobic processes. We assume R_{COM}: R_{CH_4} to be 5.

2. Model Parameterization

2.1 Initial Monte Carlo Simulations

The initial Monte Carlo simulations were conducted to obtain the proper prior range of the parameter space for peatland ecosystems based on the original parameter space for upland ecosystems:

(1) We applied the Latin Hypercube Sampler (LHS)[9]. Each random variable θ_1, …, θ_k was divided into 5000 nonoverlapping intervals based on their uniform distributions. One value from each interval was selected randomly based on the equal probability. 5000 values drawn for θ_1 was paired with 5000 values drawn for θ_2 and so forth. We repeated the same process until 5000 sets of k tuples were generated.

(2) We then drove the model using the climate data (Figure S2) from 1900 to 1990 AD. We averaged the simulated monthly C fluxes and pools (aboveground NPP, annual belowground NPP, annual total NPP, aboveground vegetation carbon, belowground vegetation carbon, and total vegetation carbon) to annual values and then averaged them from 1900 to 1990 AD. We selected the plausible parameter set based on which the simulated annual C fluxes and pools are within the uncertainty ranges of the field measurements (Table S1).

(3) The selected plausible parameter sets based on the initial Monte Carlo ensemble simulations were used as priors for peatland ecosystems.

2.2 Second Step Monte Carlo Simulations and Bayesian Inference

The Bayes' framework is:

$$\mathrm{P}(\boldsymbol{\theta}|\mathbf{V}) \propto \mathrm{P}(\mathbf{V}|\boldsymbol{\theta})\mathrm{P}(\boldsymbol{\theta})$$

where $\mathrm{P}(\boldsymbol{\theta}|\mathbf{V})$ is the posterior after the Bayesian inference conditioned on the available field measurements $\mathbf{V}$. $\boldsymbol{\theta}$ is the matrix of the parameters for adjustment. $\mathbf{V}$ is the difference matrix between the Monte Carlo simulations and the corresponding field measurements. $\mathrm{P}(\boldsymbol{\theta})$ is the prior distribution for peatland ecosystems obtained from the initial Monte Carlo ensemble simulations. $\mathrm{P}(\mathbf{V}|\boldsymbol{\theta})$ is the likelihood function, which is calculated as the function of the difference between Monte Carlo simulations and available field measurements.

We assume the monthly field measurement data are independent from month-to-month and the field measurement data follow the following error distribution[10]:

$$p_i(v_{ti}|\sigma_{ti}, \beta_i, \theta) = \omega(\beta_i)\sigma_{ti}^{-1}\exp(-c(\beta_i)\left|\frac{v_{ti}}{\sigma_{ti}}\right|^{2/(1+\beta_i)})$$

The error term follows a normal distribution when $\beta_i = 0$; a double exponential distribution when $\beta_i = 1$; a uniform distribution when β_i approaches -1. Variance σ_{ti} was assumed to be a constant during the time period $t_{i-1} < t < t_i$.

$c(\beta_i)$ and $\omega(\beta_i)$ are defined as:

$$c(\beta_i) = \left\{\frac{\Gamma\left[\frac{3(1+\beta_i)}{2}\right]}{\Gamma\left[\frac{1+\beta_i}{2}\right]}\right\}^{\frac{1}{1+\beta_i}}$$

$$\omega(\beta_i) = \frac{\left\{\Gamma\left[\frac{3(1+\beta_i)}{2}\right]\right\}^{\frac{1}{2}}}{(1+\beta_i)\left\{\Gamma\left[\frac{1+\beta_i}{2}\right]\right\}^{\frac{3}{2}}}$$

We further assume that the error term follows the following distribution:

$$p(\boldsymbol{V}|\boldsymbol{\sigma}, \boldsymbol{\beta}, \boldsymbol{\theta}) = \prod_{i=1}^{N}\prod_{t=1}^{T} \omega(\beta_i)\sigma_{ti}^{-1} exp(-c(\beta_i)\left|\frac{v_{ti}}{\sigma_{ti}}\right|^{2/(1+\beta_i)})$$

$$\propto \exp[-\sum_{i=1}^{N} c(\beta_i)\sum_{t=1}^{T}\left|\frac{v_{ti}}{\sigma_{ti}}\right|^{2/(1+\beta_i)}]$$

where $\boldsymbol{\sigma}$ and $\boldsymbol{V}$ are matrices with a size of $T \times N$. $\boldsymbol{\beta}$ is a vector with size of N,

we get the likelihood function[11]:

$$p(\boldsymbol{V}|\boldsymbol{\beta}, \boldsymbol{\theta}) \propto \prod_{i=1}^{N}[\sum_{t=1}^{T}|v_{ti}|^{\frac{2}{1+\beta_i}}]\char`^(\frac{1}{2} - T)(1+\beta_i)$$

We again applied the LHS algorithm to draw 3×1000 sets of parameters from the prior distributions for three different peatland ecosystems (pole forest, palm swamp, and open peatland) obtained from the previous Monte Carlo simulations. The observational data/ field measurement data are peat SOC accumulation rates for pole forest (PF) at (a) Aucayacu, and (b) San Jorge; palm swamp (PS) at (c) Quistococha, and (d) Charo; and open peatland (OP) at (e) Riñón in 500-year bins from 10 ka to 2014 AD. We then averaged the simulated monthly SOC accumulation rates at those sites into 500-year bins and compared them with the field measurement data. We next applied the Sampling Importance Resampling (SIR) technique[12] to calculate the importance ratio of each parameter set drawn iteratively and construct the posterior distributions for the model parameters. At last, the highest plausible parameter sets contain 3×50 parameters.

2.3 Uncertainty Quantification

To quantify the uncertainty ranges of the regional C stock simulations resulting from both the parameterization and the climate spatial interpolation, 20 sets of parameters were randomly drawn from the posterior distributions respectively for three different peatland ecosystem types (PF, PS, and OP). Based on the randomly selected parameters, all pixels in the study area were assigned with the same climate forcing data which were random combinations between temperature and precipitation, both within their uncertainty ranges from interpolation (mean temperature (25-29℃) and precipitation (2200-2900 mm) (Figure S3)). We next conducted the regional simulation to obtain the uncertainty ranges of the simulated C stocks.

Table S1. NPP and vegetation C stocks in Amazonia used for parameter optimization of P-TEM. Values in the columns "Measurement" refer to values taken from literature, whereas values in the columns "Simulation" refer to the averaged values from all selected plausible parameter sets after the initial Monte Carlo simulations.

Annual NPP or stocks[a]	Pole forest		Palm swamp		Open peatland[e]		Flooded forest		Ref
	Measurement	Simulation	Measurement	Simulation	Measurement	Simulation	Measurement	Simulation	
Aboveground NPP	985-1087[3]	-	1041-1279[8]	-	-	-	1041-1279[8]	-	[1]*ref. 13* [2]*ref. 14*
Belowground NPP	362-448[3]	-	353-434[3,c]	-	-	-	353-434[3,c]	-	[3]*ref. 15* [4]*ref. 16*
Total NPP	1347-1535[3]	1382	1394-1713	1424	-	125	1394-1713	1404	[5]*ref. 17*
Aboveground vegetation C density	5200-7160[1,4]	-	9320-10860[1,4]	-	-	-	9320-10860[1,4]	-	[6]*ref. 18* [7]*ref. 19* [8]*ref. 20*
Belowground vegetation C density	2080-28645[5,6,b]	-	3728-4344[2,d]	-	-	-	3728-4344[2,d]	-	[9]*ref. 21*
Total vegetation C density	7280-10020	9098	13048-15204	14861	-	1003	13048-15204	14153	
Leaf area index (LAI)	3.3[8]	3.0	4.2-4.4[8]	4.4	-	1.0	5.2-5.8[3]	5.4	

[a] Units for annual net primary production (NPP) are $g\ C\ m^{-2}\ yr^{-1}$. Units for above/belowground/total vegetation C density are $g\ C\ m^{-2}$. A ratio of 0.473 was used to convert vegetation biomass to carbon[7,9]. [b] A ratio of 0.39 was used to obtain belowground biomass given aboveground live biomass for Amazonian pole forest[5]. [c] A ratio of 0.34 was used to obtain the belowground NPP given aboveground NPP for palm swamp and flooded forest[3]. [d] A ratio of 0.41 was used to obtain the belowground biomass given aboveground live biomass for palm swamp and flooded forest[2]. [e]Open peatland has no available field measurement of NPP and vegetation C.

Table S2. Description of the model parameters and their final values after optimization via (1) Initial Monte Carlo simulations, and (2) Second step Monte Carlo simulations and Bayesian inference. The values are the mean values with 1.96 standard deviation from the posterior distributions after the optimization. T_{min}, T_{optmin}, T_{optmax}, T_{opt}, and T_{max} were kept unchanged after the optimization for pole forest.

Variables	Description	Unit	Pole forest	Palm swamp	Open peatland	Flooded forest	Ref
C_V	Initial[a] organic C density in vegetation	$g\ m^{-2}$	16935±2580	16983±2249	16671±1528	16671±1528	*ref. 1*
C_{S1}	Initial[a] organic C density in soil	$g\ m^{-2}$	9476±1031	9476±1031	9476±840	10204±1251	*ref. 11*
C_{max}	Maximum rate of C assimilation through photosynthesis	$g\ m^{-2}\ month^{-1}$	1089±142	1283±128	104±3	1263±109	*ref. 21*
$CFALL$	Proportion of vegetation C loss as litterfall	$g\ g^{-1}\ month^{-1}$	0.010945±0.001	0.010679±0.004	0.010664±0.001	0.008969±0.002	*ref. 22*
C_{VLmax}	Maximum canopy leaf C density	$g\ m^{-2}$	454±20	654±26	100±9	754±45	*ref. 23*
K_d	Aerobic heterotrophic respiration at 0°C	$g\ g^{-1}\ month^{-1}$	0.013617±0.0005	0.020023±0.001	0.00594±0.0003	0.004823±0.0005	*ref. 24*
T_{min}	Minimum temperature for GPP[b]	℃	10.0±1.5	10.0±1.5	10.0±1.5	10.0±1.5	
T_{optmin}	Minimum optimum temperature for GPP	℃	21.9±2.2	21.9±2.2	21.9±2.2	21.9±2.2	
T_{optmax}	Maximum optimum temperature for GPP	℃	32.7±2.9	32.7±2.9	32.7±2.9	32.7±2.9	
T_{opt}	Optimum temperature for GPP	℃	27.3±1.9	27.3±1.9	27.3±1.9	27.3±1.9	
T_{max}	Maximum temperature for GPP	℃	37.0±3.1	37.0±3.1	37.0±3.1	37.0±3.1	

[a] Initial values are the default values of vegetation C and SOC in the first time step during the simulation. [b] GPP: gross primary production.

Table S3. Description of peatland sites used for establishing basal ages for pole forest, palm swamp, and open peatland. The basal ages were taken from[24,25], whereas the other values were from the online supplementary material (table 1) of[16].

Site	Long (°W)	Lat (°S)	Basal age (cal year BP)	Mean bulk density (g cm^{-3})	Mean peat thickness (m)	Mean C content (%)	Mean basal age (cal year BP)
Pole forests							~4000
Aucayacu (forested)	74.384	3.935	8870±110	0.108	4.63	49	
San Jorge (*M. flexuosa* palm swamp and forested)	73.189	4.058	2945±65	0.112	2.92	44	
Roca Fuerte (forested)	74.823	4.436	5170±120	0.073	3.82	52	
Palm swamps							~2000
Quistococha (*M. flexuosa* palm swamp and forested)	73.318	3.837	2335±15	0.095	2.44	47	
Charo (Mixed *M. flexuosa* palm swamp)	73.254	4.270	672±12.5	-	1.26	-	
Buena Vista del Maquia (*M. flexuosa* palm swamp)	74.720	6.207	-	0.088	1.21	38	
San Roque (*M. flexuosa* palm swamp)	74.622	4.540	7705±35	0.161	3.53	42	
Open peatlands							~1600
Riñón (open savanna)	74.001	4.900	1615±75	0.06	3.55	49	
Maquía (open, scattered *M. flexuosa* palm swamp)	74.808	6.323	1975±30	0.074	3.88	44	

Table S4. Analysis of variance table (ANOVA) of the multi-variate linear regression between annual mean NPP and climate variables for the historical simulation at Aucayacu site.

Source	Sum of Squares	Degree of Freedom	F-value	Pr (>F)
Annual Temperature (℃)	15.785142	1.0	18.117638	2.095649e-05
Annual Precipitation (mm)	18.340884	1.0	21.051029	4.526578e-06
Annual Volumetric Soil Moisture (VSM, %)	372.013772	1.0	426.984481	6.340108e-93
Temperature×Precipitation	17.451831	1.0	20.030605	7.705596e-06
Residual	8708.226683	9995.0		

Table S5. The coefficients, standard errors, and the 95% confident intervals of the parameters in the regression model (without feature normalization).

	Coefficient	**Standard Error**	**95% CI**
Intercept	-67.9910	23.792	(-114.628, -21.354)
Annual Temperature (℃)	3.7166	0.873	(2.005, 5.428)
Annual Precipitation (mm)	0.4696	0.102	(0.269, 0.670)
Annual Volumetric Soil Moisture (VSM, %)	0.6014	0.029	(0.544, 0.658)
Temperature×Precipitation	-0.0168	0.004	(-0.024, -0.009)

Table S6. Analysis of variance table (ANOVA) of the multi-variate linear regression between annual mean NPP and climate variables (Annual temperature and precipitation) in RCP 2.6, RCP 4.5, and RCP 8.5 scenarios. F-value indicates the importance of each climate variable.

Scenarios	**Source**	**F-value**
RCP 2.6	Annual Temperature (℃)	15.498204
	Annual Precipitation (mm)	17.902754
RCP 4.5	Annual Temperature (℃)	12.099724
	Annual Precipitation (mm)	11.833428
RCP 8.5	Annual Temperature (℃)	7.323143
	Annual Precipitation (mm)	8.410239

Table S7. Simulated and field-measured total C stocks of SOC and vegetation C for pole forest, palm swamps, open peatlands, non-peatland (flooded forest), and the totals in the PMFB. Values in the columns "Measurement" refer to values from[16], whereas values in the columns "Simulation" refer to the results obtained from the P-TEM. The uncertainty ranges of the "simulation" are from the uncertainty of the parameterization plus the uncertainty from the climate data interpolation.

Ecosystem type		Area (km^2)		Soil organic C (Pg)		Vegetation C (Pg)		Total C stock (Pg)	
		Simulation	Measurement	Simulation	Measurement	Simulation	Measurement	Simulation	Measurement
Pole forest	Mean	2909	3686	0.511	0.494	0.0216	0.030	0.532	0.524
	Range	-	±810	0.269-0.646	0.110-1.131	0.0215-0.0218	0.009-0.074	0.316-0.723	0.138-1.174
Palm swamps	Mean	25069	27732	2.779	2.073	0.318	0.263	3.097	2.336
	Range	-	±1101	1.459-4.376	0.012-5.738	0.316-0.349	0.138-0.355	1.775-4.725	0.268-5.997
Open peatlands	Mean	3915	4181	0.229	0.277	~0	0	0.229	0.277
	Range	-	±222	0.105-0.322	0.034-0.974	~0	0	0.105-0.322	0.034-0.974
Non-peatland	Mean	47429	-	0.403	-	0.764	-	1.167	-
	Range	-	-	0.375-0.433	-	0.759-0.768	-	1.134-1.201	-
Total (peatlands)	Mean	31893	35600	3.519	2.844	0.34	0.293	3.859	3.137
	Range	-	±2133	1.833-5.344	-	0.338-0.369	-	2.171-5.713	0.440-8.145
Total (peatlands+non-peatland)	Mean	79322	-	3.922	-	1.104	-	5.026	-
	Range	-	-	2.208-5.777	-	1.097-1.137	-	3.305-6.914	-

Table S8. Comparison between our model simulation of vegetation C density change and SOC density change in the 21st century for peatlands and non-peatland and other model simulations for forest dieback (non-peatland vegetation C and SOC density change) in northwestern Amazonia areas. The density changes are the total C stock changes (Table 1) divided by the corresponding area (Table S7) of peatlands and non-peatland ecosystems.

Models	Ecosystem type	Vegetation C density change (kg C m^{-2})	SOC density change (kg C m^{-2})	Ref
LPJmL	Non-peatland	+0.6~-1.2	~	*Ref. 26*
HadCM3 coupled with HadOCC and TRIFFID	Non-peatland	-9.49	-3.88	*Ref. 27*
P-TEM (RCP 2.6 and RCP 8.5)	Non-peatland	-0.45 (+0.23~--1.13)	**-1.55** (+0.18~-3.28)	
	Peatland	-0.34 (+0.19~-0.86)	**-6** (+3.15~-15.2)	
			$\frac{\textbf{Peatland}}{\textbf{Non peatland}} = \mathbf{3.9}$	
P-TEM (precipitation -5% and -15%)	Non-peatland	-0.49 (+0.19~-1.17)	**-1.61** (+0.13~--3.35)	
	Peatland	-0.42 (+0.17~--1)	**-9.31** (+1.89~-20.5)	
			$\frac{\textbf{Peatland}}{\textbf{Non peatland}} = \mathbf{5.8}$	

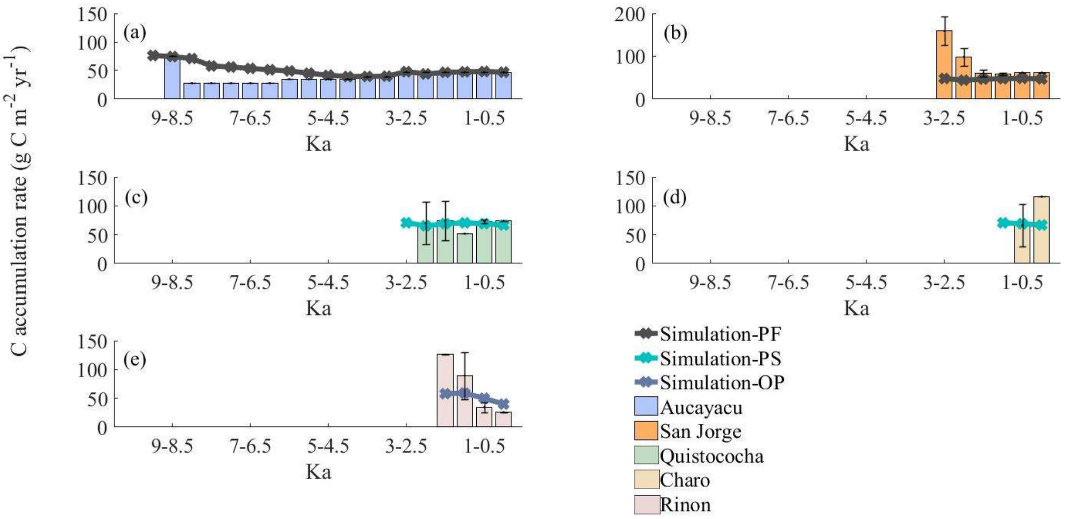

Figure S1. Comparison between simulated (this study) and measured[24,25] SOC accumulation rates of pole forest (PF) at (a) Aucayacu, and (b) San Jorge; palm swamp (PS) at (c) Quistococha, and (d) Charo; and open peatland (OP) at (e) Riñón in 500 year bins from 10 ka to 2014 AD. Colors of lines represent simulations for different vegetation types using different parameters. Note that the starting ages of the model regional transient simulations are: 4 ka for PF, 2 ka for PS, and 1.6 ka for OP (see Table S3 for mean basal age).

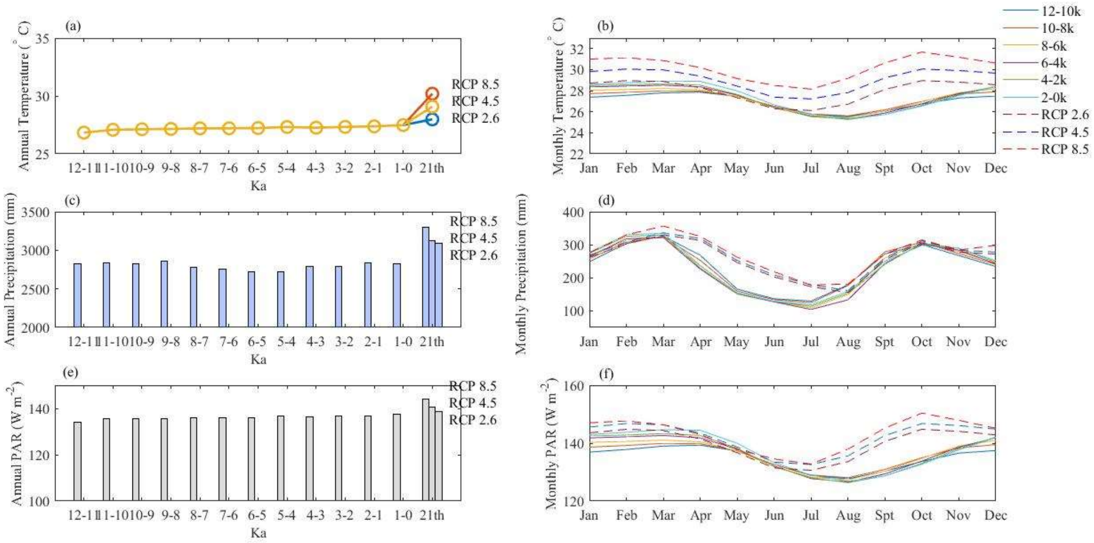

Figure S2. Climate forcing of annual (a) temperature, (c) precipitation, (e) photosynthetically active radiation (PAR) and monthly mean (b) temperature, (d) precipitation, and (f) PAR for PMFB[28-30].

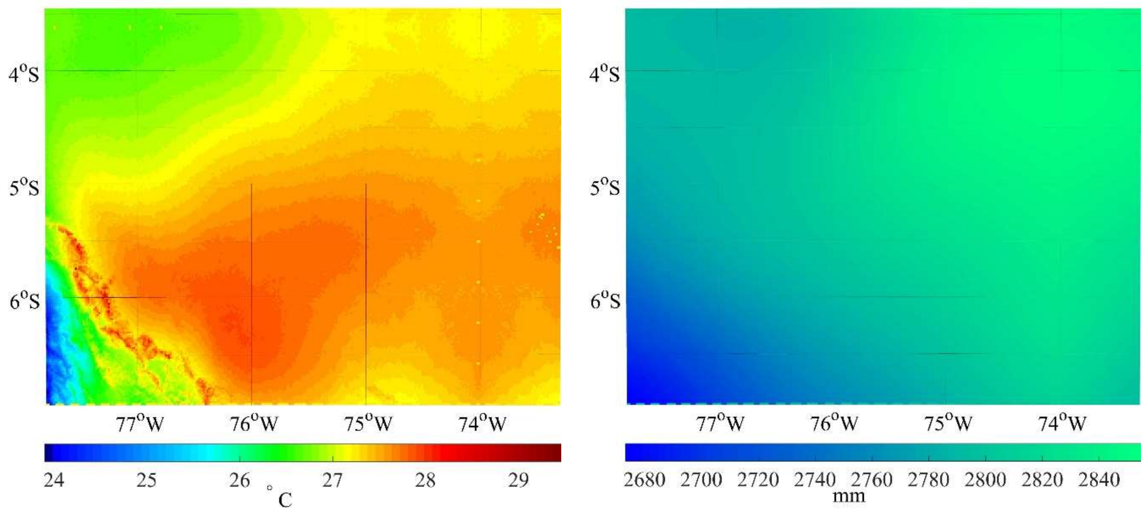

Figure S3. Interpolated (a) mean temperature and (b) mean annual precipitation distribution from 4 ka to 2014 AD of the study area.

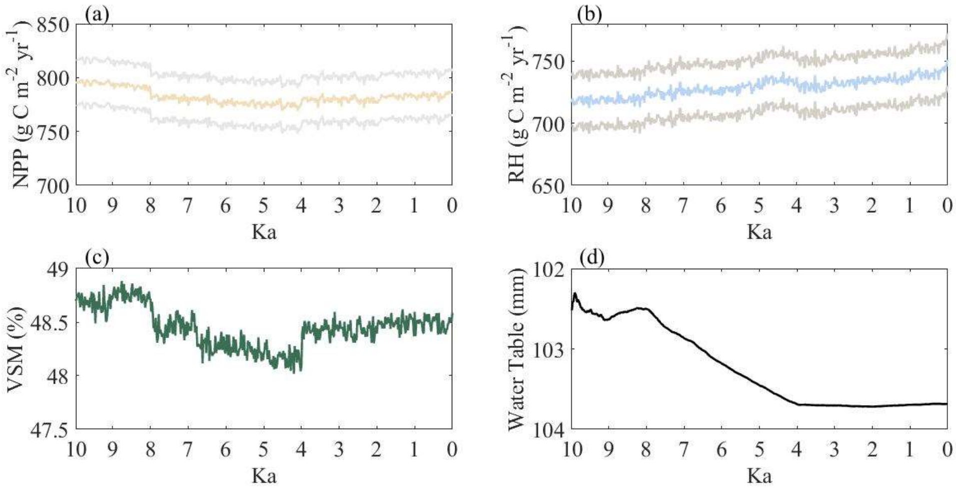

Figure S4. Simulated (a) net primary production (NPP), (b) heterotrophic (aerobic+anaerobic) respiration (R_H), (c) volumetric soil moisture (VSM), and (d) water-table depth (WTD) at Aucayacu from 10 ka to 2014 AD (based on averages of 20 years). Grey lines in (a) and (b) indicate the upper and lower uncertainty range resulting from the Bayesian inference.

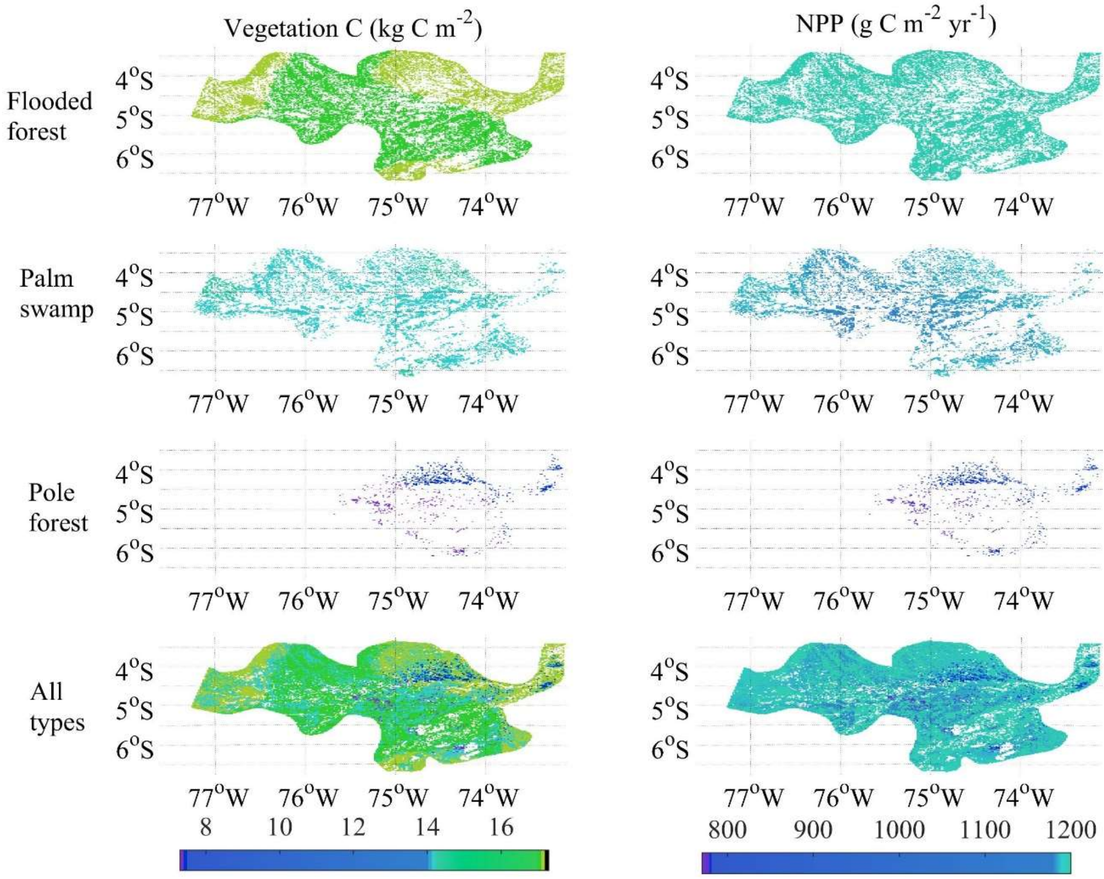

Figure S5. Current (2014 AD) vegetation C (above+belowground) density and mean historic NPP of flooded forest, palm swamp, pole forest and their combination in the PMFB. NPP is the average from 4 ka to 2014 AD. Open peatlands with minimal vegetation C and NPP are not shown. (Figure produced using MATLAB R2016a; https://www.mathworks.com/products/new_products/release2016a.html).

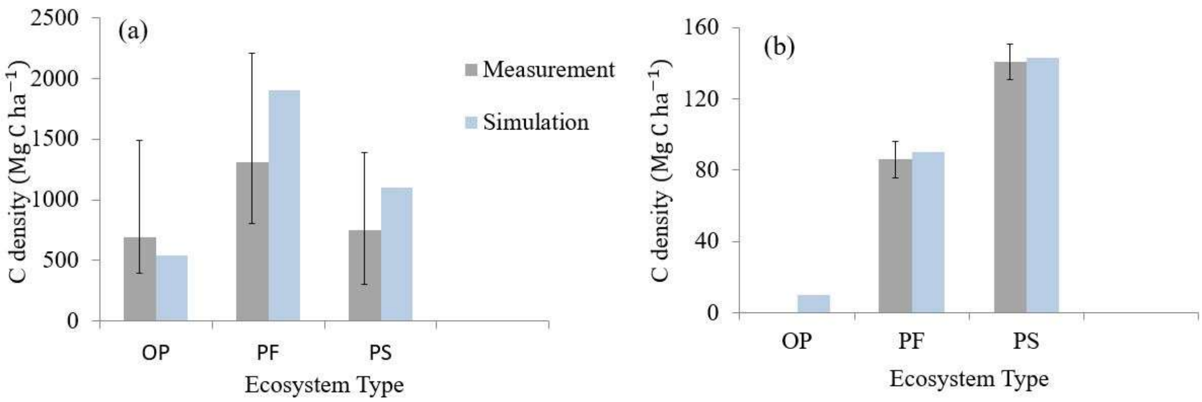

Figure S6. Simulated density of (a) SOC and (b) vegetation C for pole forest (PF), palm swamp (PS), and open peatland (OP) versus field measurements of[4]. A ratio of 0.473 was used to convert vegetation biomass to C[6,19]. A ratio of 0.39 was used to obtain belowground biomass given aboveground live biomass for PF[17]. A ratio of 0.41 was used to obtain the belowground biomass given aboveground live biomass for PS[14]. OP has no measurement of vegetation C density.

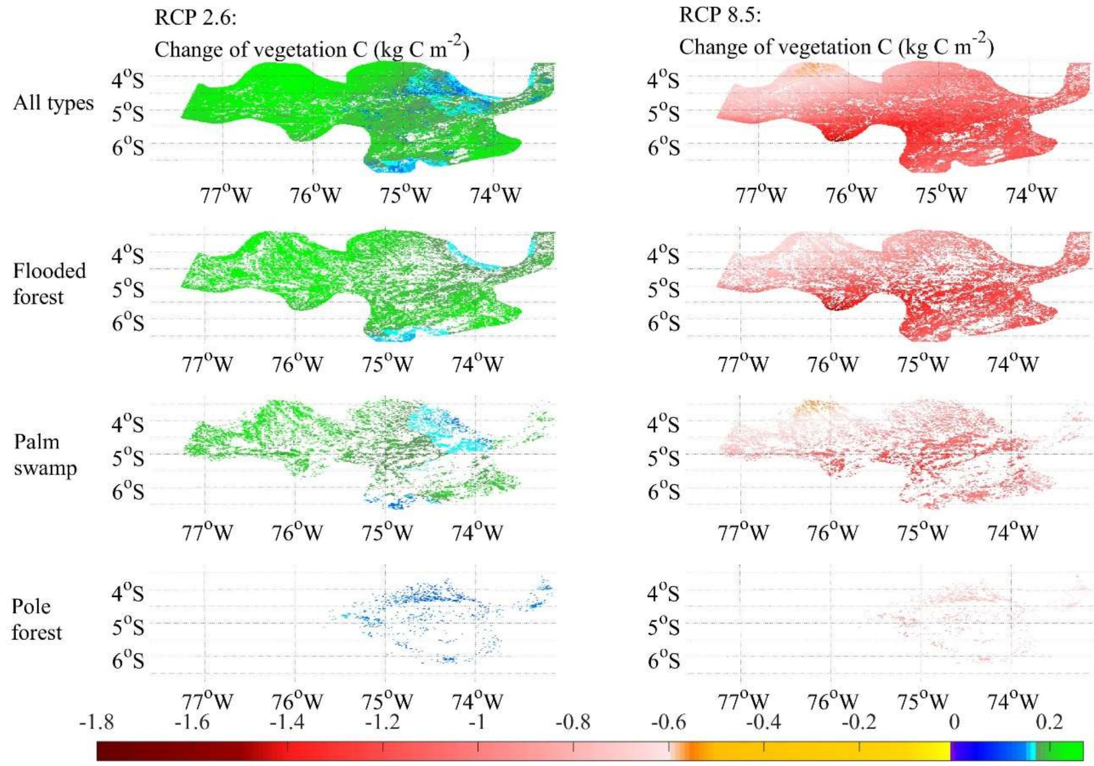

Figure S7. Changes of vegetation C (above+belowground) density from 2014 to 2100 AD under RCP 2.6 and RCP 8.5 future climate scenarios of flooded forest, palm swamp, pole forest, and their combination in the PMFB. Open peatlands with minimal vegetation C and NPP are not shown. Blue and green represent the vegetation C accumulation. Yellow and red represent the vegetation C loss. (Figure produced using MATLAB R2016a; https://www.mathworks.com/products/new_products/release2016a.html).

Reference

1. Wang, S. et al. Quantifying peat carbon accumulation in Alaska using a process-based biogeochemistry model. Journal of Geophysical Research. Biogeosciences, 121(8), 2172-2185 (2016a).

2. Zhuang, Q. et al. Carbon cycling in extratropical terrestrial ecosystems of the Northern Hemisphere during the 20th Century: A modeling analysis of the influences of soil thermal dynamics. Tellus, 55B, 751-776, 2003 (2003)

3. Zhuang, Q. et al. Influence of changes in wetland inundation extent on net fluxes of carbon dioxide and methane in northern high latitudes from 1993 to 2004. Environmental Research Letters, 10(9), 095009 (2015).

4. Tang, J. et al. Quantifying wetland methane emissions with process-based models of different complexities. Biogeosciences, 7(11), 3817-3837 (2010).

5. Keller, J. K. and Bridgham, S. D. Pathways of anaerobic carbon cycling across an ombrotrophic-minerotrophic peatland gradient, Limnol. Oceanogr., 52, 96 – 107 (2007).

6. Raich, J. W. et al. Potential Net Primary Productivity in South America: Application of a Global Model. Ecological Applications, 1: 399-429. doi:10.2307/1941899 (1991).

7. Granberg, G. et al. A simple model for simulation of water content, soil frost, and soil temperatures in boreal mixed mires, Water Resour. Res., 35(12), 3771–3782, doi:10.1029/1999WR900216 (1999).

8. Zhuang, Q. et al. Methane fluxes between terrestrial ecosystems and the atmosphere at northern high latitudes during the past century: A retrospective analysis with a process‐based biogeochemistry model. Global Biogeochemical Cycles, 18(3) (2004).

9. Iman, R. L. et al. An investigation of uncertainty and sensitivity analysis techniques for computer models, Risk Anal., 8, 71 – 90 (1988).

10. Thiemann, M. et al. Bayesian recursive parameter estimation for hydrologic models, Water Resour. Res., 37(10), 2521 – 2536 (2001).

11. Tang, J., & Zhuang, Q. A global sensitivity analysis and Bayesian inference framework for improving the parameter estimation and prediction of a process‐based Terrestrial Ecosystem Model. Journal of Geophysical Research: Atmospheres, 114(D15) (2009).

12. Skare, Ø. et al. Improved sampling importance resampling and reduced bias importance sampling, Scand. J. Stat., 30, 719 – 737 (2003).

13. Baker, T. R. et al. Variation in wood density determines spatial patterns in Amazonian forest biomass. Global Change Biology, 10: 545–562. doi:10.1111/j.1365-2486.2004.00751.x (2004).

14. Goodman, R. C. et al. Amazon palm biomass and allometry. Forest Ecology and Management, 310, 994-1004 (2013).

15. Del Aguila-Pasquel, J. et al. The seasonal cycle of productivity, metabolism and carbon dynamics in a wet aseasonal forest in north-west Amazonia (Iquitos, Peru). Plant Ecology and Diversity, 7, 71–83 (2014).

16. Draper, F. C. et al. The distribution and amount of carbon in the largest peatland complex in Amazonia. Environmental Research Letters, 9(12), 124017 (2014).

17. Houghton, R. A. et al. The spatial distribution of forest biomass in the Brazilian Amazon: a comparison of estimates. Global Change Biology, 7(7), 731-746 (2001).

18. Malhi, Y. et al. The regional variation of aboveground live biomass in old-growth Amazonian forests. Global Change Biology 12, 1107–1138 (2006).

19. Martin, A. R., & Thomas, S. C. A reassessment of carbon content in tropical trees. PloS one, 6(8), e23533 (2011).

20. Nebel, G. et al. Litter fall, biomass and net primary production in flood plain forests in the Peruvian Amazon. Forest Ecology and Management, 150(1), 93-102 (2001).

21. McGuire, A. D. et al. Interactions between carbon and nitrogen dynamcs in estimating net primary productivity for potential vegetation in North America. Global Biogeochemical Cycles, 6(2), 101-124 (1992).

22. Tang, J., & Zhuang, Q. Equifinality in parameterization of process-based biogeochemistry models: A significant uncertainty source to the estimation of regional carbon dynamics. Journal of Geophysical Research: Biogeosciences, 113(G4) (2008).

23. Zhuang, Q. et al. Modeling soil thermal and carbon dynamics of a fire chronosequence in interior Alaska. Journal of Geophysical Research: Atmospheres, 107(D1) (2002).

24. Lähteenoja, O. et al. Amazonian peatlands: an ignored C sink and potential source. Global Change Biology, 15(9), 2311-2320 (2009a).

25. Lähteenoja, O. et al. The large Amazonian peatland carbon sink in the subsiding Pastaza-Marañón foreland basin, Peru. Global Change Biology, 18(1), 164-178 (2012).

26. Cox, P. M. et al. Amazonian forest dieback under climate-carbon cycle projections for the 21st century. Theoretical and applied climatology, 78(1), 137-156 (2004).

27. Rammig, A. et al. Estimating the risk of Amazonian forest dieback. New Phytologist, 187: 694-706. doi:10.1111/j.1469-8137.2010.03318.x (2010).

28. Carlson, A. E. et al. Modeling the surface mass-balance response of the Laurentide Ice Sheet to Bølling warming and its contribution to Meltwater Pulse 1A. Earth and Planetary Science Letters, 315, 24-29 (2012).

29. Mitchell, T. D. et al. comprehensive set of high-resolution grids of monthly climate for Europe and the globe: the observed record (1901–2000) and 16 scenarios (2001–2100). Tyndall centre for climate change research working paper, 55(0), 25 (2004).

30. Change, I. C. Mitigation of Climate Change. Contribution of Working Group III to the Fifth Assessment Report of the Intergovernmental Panel on Climate Change (IPCC). Cambridge University Press, Cambridge, UK and New York, NY (2014).